Tuning Anode Morphology Through Strategic Cathode (Global) Current Manipulation: A Modeling and Simulation Study

To cite this article: Tushar K. Telmasre *et al* 2025 *ECS Adv.* **4** 030503

ECS Advances, 2025 **4** 030503

Tuning Anode Morphology Through Strategic Cathode (Global) Current Manipulation: A Modeling and Simulation Study

Tushar K. Telmasre,[1,*,=] Lubhani Mishra,[1,2,*,=] Wen-Yang Jao,[3,4] Aakriti Aggarwal,[4] J.-X. Kent Zheng,[1,4,*] and Venkat R. Subramanian[1,2,5,,z]**

[1]*Materials Science and Engineering, The University of Texas at Austin, Austin, Texas 78712, United States of America*
[2]*Walker Department of Mechanical Engineering, The University of Texas at Austin, Austin, Texas 78712, United States of America*
[3]*Department of Chemical Engineering, National Tsing Hua University, Hsin-Chu 300044, Taiwan*
[4]*McKetta Department of Chemical Engineering, The University of Texas at Austin, Austin, Texas 78712, United States of America*
[5]*Affiliate Faculty, Oden Institute for Computational Science and Engineering, The University of Texas at Austin, Austin, Texas 78712, United States of America*

The evolution of metal anode–electrolyte interfaces critically impacts the safety and performance of metal anode batteries. We present a two-dimensional moving boundary model that simulates zinc anode morphology under high discharge–low charge (HD–LC) and low discharge–low charge (LD–LC) protocols. The model predicts interface flattening with HD–LC cycling, validated by symmetric cell experiments. LD–LC, however, does not show any change in interface morphology. Our findings highlight that cathode current modulation can effectively control interfacial morphology, offering a simple, yet powerful strategy to suppress dendrite growth and enhance metal anode battery safety through current control.
 [DOI: 10.1149/2754-2734/ae06b5]

Manuscript submitted July 24, 2025; revised manuscript received September 10, 2025. Published September 29, 2025.

Supplementary material for this article is available online

Battery Management Systems (BMS) are indispensableforthe usage of batteries in any practical application today. They are important for safe operation, utilization and real time state estimation of batteries. Sophisticated BMS are also capable of controlling battery operations to reduce battery degradation and improve life. Among contemporary energy storage technologies, lithium-ion (Li-ion) batteries have been the primary focus of BMS development over recent decades owing to their high stability and commercial maturity.[1] These systems are typically structured around a hierarchy of modeling approaches spanning from empirical models, continuum models to interfacial level atomistic models.[1,2] Sophisticated BMS can thus enable faster charging protocols while actively preventing degradation phenomena such as dendrite growth, lithium (Li) plating, and particle fracture in Li-ion batteries.[3]

In contemporary era, metal anode batteries are emerging to be the leading contenders among the "Beyond Li-ion" technologies.[4–7] The first type of rechargeable electrochemical batteries were Li metal anode batteries. In contrast to intercalation-based batteries (Li-ion, Na-ion, etc.) metal anode batteries function through successive plating and stripping cycles during charging and discharging, respectively. This mechanism involves continuous changes at the anode-electrolyte interface during operation. This results in a physical system that involves complex interplay of electrochemical and physical processes at the interface such as surface tension, reaction kinetics and thermodynamics, concentration and potential variations etc. that often results in uneven deposition/stripping, dendrite formation, dead metal deposition, and other undesired phenomena. From a modeling perspective this manifests itself as a nonlinear moving boundary problem that presents significant mathematical challenges.[8] To model the interfacial dynamics effectively, advanced mathematical techniques are necessary such as the ones that account for deforming geometries, evolving coordinate frames, and require adaptive meshing strategies.[9,10] Current modeling approaches, including phase-field models and Arbitrary Lagrangian-Eulerian (ALE) methods, attempt to address these challenges with varying degrees of success. Further transitioning from merely simulating to control of such metal anode systems during operation presents a separate set of challenges. Although the literature includes numerous modeling and simulation studies, there remains a notable absence of robust, multi-dimensional frameworks capable of dynamically adjusting the applied current to steer the morphology of the metal anode - electrolyte interface. This gap is particularly important, as controlling the interface could play a key role in preventing dendrite formation and improving the overall safety and efficiency of these battery systems. The creation of such predictive, controllable models is still an open and highly significant research frontier.

In this work, we present a model that shows the capability to control the evolution of interface at the metal anode by manipulating the cathode (global) current. We have developed a simple moving boundary model that simulates the liquid phase potential distribution within the electrolyte domain. This potential distribution in turn affects the current distribution at the anode-electrolyte interface governed by Butler-Volmer kinetics influencing the rate of movement of the interface. Our recent experimental and modeling study on dissolution at zinc metal anodes showed that the higher discharge rates dissolved the interface more at the tip of the dendrite compared to the lower discharge rate for a single cycle.[11] In this work, the model is extended for cycling studies to simulate the plating and stripping behavior in zinc anodes where an initial seed is assumed as shown in Fig. 1a (replicating the tip of an initial dendrite). We have found that High Discharge/Low Charge current protocol almost flattens the dendrite in 20 cycles compared to the same current (Low Discharge/Low Charge) current protocol, which results in almost no change of the initial seed after cycling. Further, we conducted experimental cycling studies on zinc anode batteries using a three-electrode symmetric cell setup. In the presence of $ZnCl_2$ aqueous electrolyte, HD-LC and LD-LC current protocols were applied for 20 cycles. The experimental results closely aligned with the predictions of the modeling study. A noticeable reduction in dendrite height was observed at the end of 20 cycles under the HD-LC protocol, consistent with model predictions. In contrast, the LD-LC protocol led to the formation of dead zinc over the same number of cycles. Capturing such behavior is likely beyond the scope of the current electrolyte potential evolution model, which does not incorporate the complex physics required to simulate dendrite

[=]Equal Contribution.
[*]Electrochemical Society Member.
[**]Electrochemical Society Fellow.
[z]E-mail: venkat.subramanian@utexas.edu

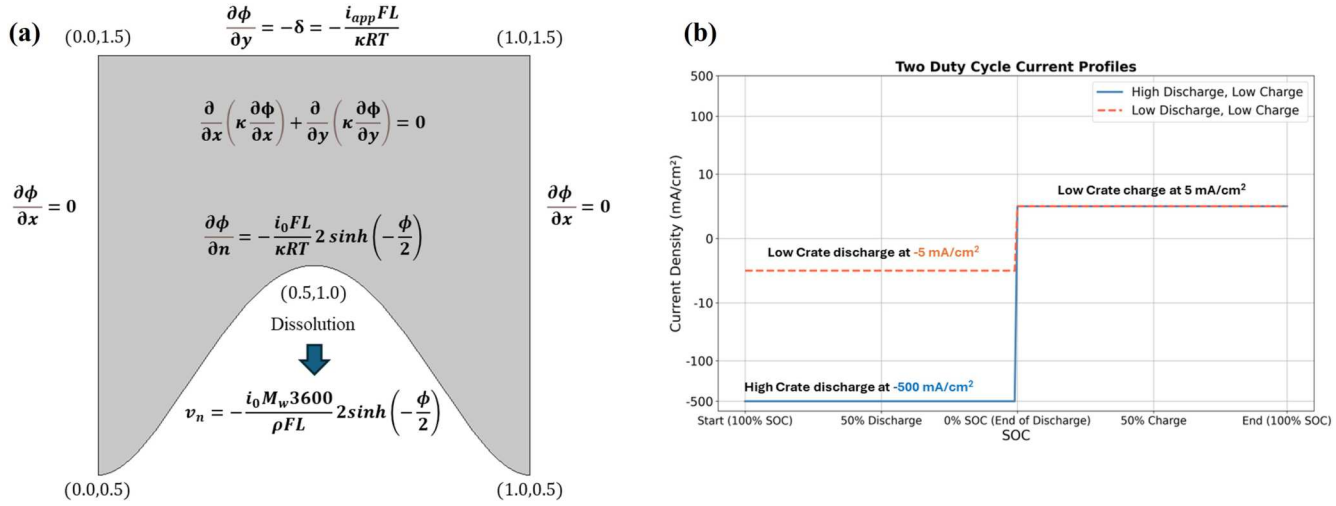

Figure 1. (a) Model Geometry in 2D. The geometry represents the electrolyte domain where potential distribution is modeled. The lower curvature represents the dendrite i.e. the anode-electrolyte interface. (b) The two current protocols applied to the simulation. It involves two different discharge rates followed by a lower current charge cycle (HD-LC vs LD-LC). These duty cycles are repeated for 20 cycles.

fracture, deformation, or mechanical detachment phenomena. It is also noted that the simulation domain represents only a tiny region at the tip of the dendrite (supporting Fig. S1) and does not represent the whole of the dendrite as shown in experiments, but it provides sufficient insight into the evolution of electrode-electrolyte interface during plating/stripping operation. Thus, our findings show that a simple model that simulates the current distribution at the anode interface is powerful enough to show changes in morphology at the anode interface. This work makes a strong case for the possibility of global current based control for performance and safety improvements in case of metal anode batteries. Very few simulation studies we have come to know of till today have explored the use of higher currents to control the evolution of anode-electrolyte interface. This insight makes this study a novel effort in this direction.

Model Description and Experimental Setup

Model description.—Figure 1a presents the schematic geometry of the model (scaled) used in the paper. We are considering the zinc anode system with an initial seed in the form of a polynomial function i.e. the zinc anode-electrolyte interface is represented with a polynomial function as: $\frac{L}{2} + 8_{*}L\left(\left(\frac{x}{L}\right)^2\right)_{*}\left(1-\left(\frac{x}{L}\right)\right)^2$. Two current protocols are tested for the morphology control, viz., 1) High current discharge (-500 mA cm^{-2})—Low current charge (5 mA cm^{-2}) (HD-LC) 2) Low current discharge (-5 mA cm^{-2})—Low current charge (5 mA cm^{-2}) (LD-LC). A two-dimensional formulation is employed to model the system, as one-dimensional models fail to capture the geometric dependencies necessary for differentiating between the two protocols. In 1D, both protocols converge to similar outcomes, whereas the 2D formulation reveals that interface evolution is sensitive to current magnitude and spatial effects. Notably, under the LD–LC protocol, the interface returns to the original seed position, indicating insufficient flattening. These observations confirm that, at least a two-dimensional representation is essential for accurately capturing the morphological dynamics of the system and for ensuring the numerical robustness required to study current-induced shape evolution at the anode–electrolyte interface.

The scaled model equations are explained below:

Governing equation:

$$\frac{\partial}{\partial x}\left(\kappa\frac{\partial \phi}{\partial x}\right)+\frac{\partial}{\partial y}\left(\kappa\frac{\partial \phi}{\partial y}\right)=0 \qquad [1]$$

Boundary conditions

At $x = 0$ (left wall) and $x = 1$ (right wall) for all y

$$\frac{\partial \phi}{\partial x} = 0 \qquad [2]$$

At $y = 1.5$ (top) for all x

$$\frac{\partial \phi}{\partial y} = -\delta = -\frac{iappFL}{\kappa RT} \qquad [3]$$

At $y = \frac{L}{2} + 8_{*}L\left(\left(\frac{x}{L}\right)^2\right)_{*}\left(1-\left(\frac{x}{L}\right)\right)^2$ (Anode-electrolyte interface)

$$\frac{\partial \phi}{\partial n} = -\frac{i_0 FL}{\kappa RT}2\sinh\left(-\frac{\phi}{2}\right) \qquad [4]$$

The moving boundary velocity is given by:

$$v_n = -\frac{i_0 M_w 3600}{\rho FL}2sinh\left(-\frac{\phi}{2}\right) \qquad [5]$$

The model is in non-dimensional form where the 2D domain is scaled with respect to the total domain length in x-direction (L). The model solves liquid phase potential distribution in the electrolyte domain (Eq. 1) where at the top boundary (cathode/electrolyte interface) a uniform applied current density is assumed. The side walls of the domain have zero potential flux conditions (Eq. 2) and Butler Volmer kinetics condition is applicable at the anode-electrolyte interface (Eq. 4). The velocity of the boundary, v_n is defined as given by (Eq. 5), proportional to the current density at the interface (i_{BV}). The cycle initiates with the discharge condition resulting in the stripping of the dendritic seed and hence movement of anode electrolyte interface is in the negative y-direction followed by charging (deposition).

Experimental setup.—The experiment was conducted using a cuvette open cell with a 3-electrode symmetric cell setup. The working, reference and counter electrodes were all Zn foil purchased from MSE supplies (99.9%, 0.1 mm thickness). The electrolyte chosen was 10 M $ZnCl_2$ in an aqueous solution, prepared within vials under ambient air using $ZnCl_2$ (98%–100.5%, puriss. grade) and deionized water. The electrochemical measurements were conducted using an SP-200 potentiostat (Biologic, France) under constant current conditions. For each cell tested, initial dendrite growth was conducted under mass-transport limited regime at

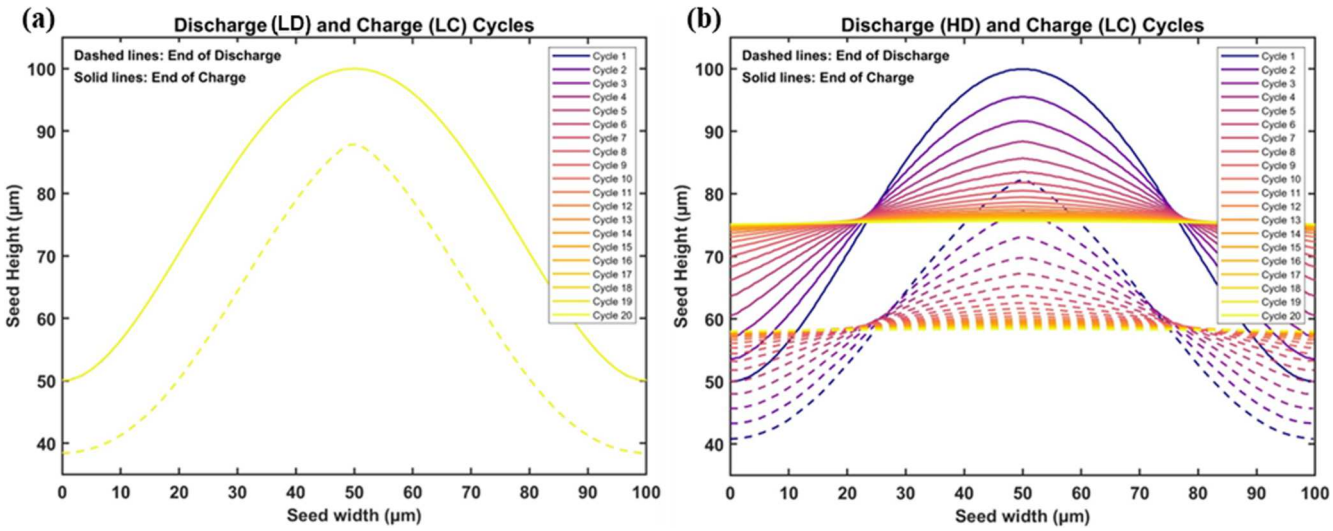

Figure 2. Movement of the anode-electrolyte interface over successive charge and discharge cycles of (a) LD-LC protocol where there is no effective movement of the interface and a significant change in the dendrite morphology over cycles (b) HD-LC protocol where higher dissolution (stripping) is observed at the tip during a high-rate discharge than what is plated during a lower current charge cycle. This results in progressive flattening of the anode-electrolyte interface. Cycling starts with discharge and the total amount of charge remains the same.

3 * J_1 (mA/cm^2)(as given in S1 of[12]) or 861 mA cm^{-2} for a total capacity of 8.61 mAh. Subsequently, for the HD-LC protocol, plating was conducted at 5 mA cm^{-2} and stripping was conducted at 500 mA cm^{-2}. Similarly, the LD-LC protocol was conducted after the initial dendrite growth at 5 mA cm^{-2} plating and stripping current densities. Each plating and stripping protocol were conducted with a total capacity of 1 mAh. Each protocol was run for 20 cycles in total. Synchronous in-operando visualization was conducted using a high-resolution digital microscope (UMH210-11, AmScope).

Results and Discussion

Simulation study.—As discussed above, High Discharge-Low Charge (HD-LC) and Low Discharge-Low Charge (LD-LC) current protocols as shown in Fig. 1b were applied to simulation and experiments. The model parameters and current values are given in Table I. Figures 2a and 2b present the plot for the stripping/plating behavior when the LD-LC current protocol and HD-LC current protocols were applied to the system respectively. For both the current protocols, during discharge, the zinc metal is stripped from the anode surface hence the boundary moves downwards depicting dissolution (stripping) whereas during charging, deposition (plating) takes place and the boundary moves up. In Fig. 2a, for the LD-LC current protocols, the same amount of stripping and plating is observed in each cycle. Therefore, there is no effective movement of the anode interface seen over the 20 cycles simulated. However, as seen in Fig. 2b, a higher current during the discharge cycle results in more stripping of the metal seed at the tip as compared to the uniform plating observed in subsequent charge step. This eventually results in lowering the interface position at the end of successive cycles resulting in near complete flattening of initial seed. Point to note here is that, the cycling protocols are designed such that, equal amount of charge is transferred to the system in each discharge and charge step i.e. a high current discharge (HD) step of 500 mA cm^{-2} is run for 36 s and a low current charge (LC) step of 5 mA cm^{-2} is run for 3600 s keeping the total amount of charge transferred/withdrawn the same.

Table I. The values of parameters.

Parameter	Value
Length of domain (L)	100 μm
Applied current density High (i_{app})	500 mA cm^{-2}
Applied current density Low (I_{app})	5 mA cm^{-2}
Molecular weight of zinc (Mw)	65.38 e–3 kg mol^{-1}
Density (ρ)	7140 kg m^{-3}
Electrolyte conductivity (κ)	5 S m^{-1}
Exchange current density (i0)	50 A m^{-2}
Univeral gas constant (R)	8.314 J mol.K^{-1}
Operating temperature (T)	298.15 K
Faraday's constant (F)	96485 C mol^{-1}

Experimental study.—The in-operando visualization reveals that during a single plating and stripping cycle of the HD-LC protocol there is an observable recession in the dendritic growth front. See supplementary videos 1∼2. As shown in Fig. 3a (top), the initial dendritic growth front was at the white line after plating, but after a high-rate discharge of the same capacity, the dendritic growth front recedes, as marked by the green line. However, in the LD-LC protocol, there is no visible change in the height of the dendritic growth front. This behavior continues for the initial cycles. After 20 plating and stripping cycles, more stark differences are visible. After 20 cycles of the HD-LC protocol, the dendrites have significantly shortened as visible in Fig. 3a (bottom), supporting the simulation results of a flattening interface and leading towards a uniform profile. On the other hand, the LD-LC protocol demonstrates unexpected behavior; the dendrites backbones weaken due to perceived metal orphaning during the low discharge cycles. This process progressively builds up until the structure becomes weak as shown in Fig. 3b. While in this case it is more difficult to draw conclusions solely on the progression or regression of the dendritic growth front, it is clear that the HD-LC protocol performs better over long-term cycling by flattening yet maintaining structure. This interfacial instability may be explained by the framework based on Wagner number (Wa) as described in our earlier work.[11] In contrast, the LD-LC protocol leads to weaker dendritic structures, leading to metal orphaning (i.e. dead metal) which would lead to reduction in reversibility.

Thus, it is apparent, from both modeling and experimental studies, the HD-LC protocol results in reduction in the height of the dendrite structure. Focusing on the simulation studies to find the theoretical underpinnings of these results, it is observed that as the cycling progresses, each discharge cycle pulls the interface down (stripping) but it does not recover completely during the low current charge step (plating), resulting in an overall drop in seed height. As can be seen from Fig. 2b, over time, this repeated discharge and charge cycle results in flattening of the interface eventually resulting

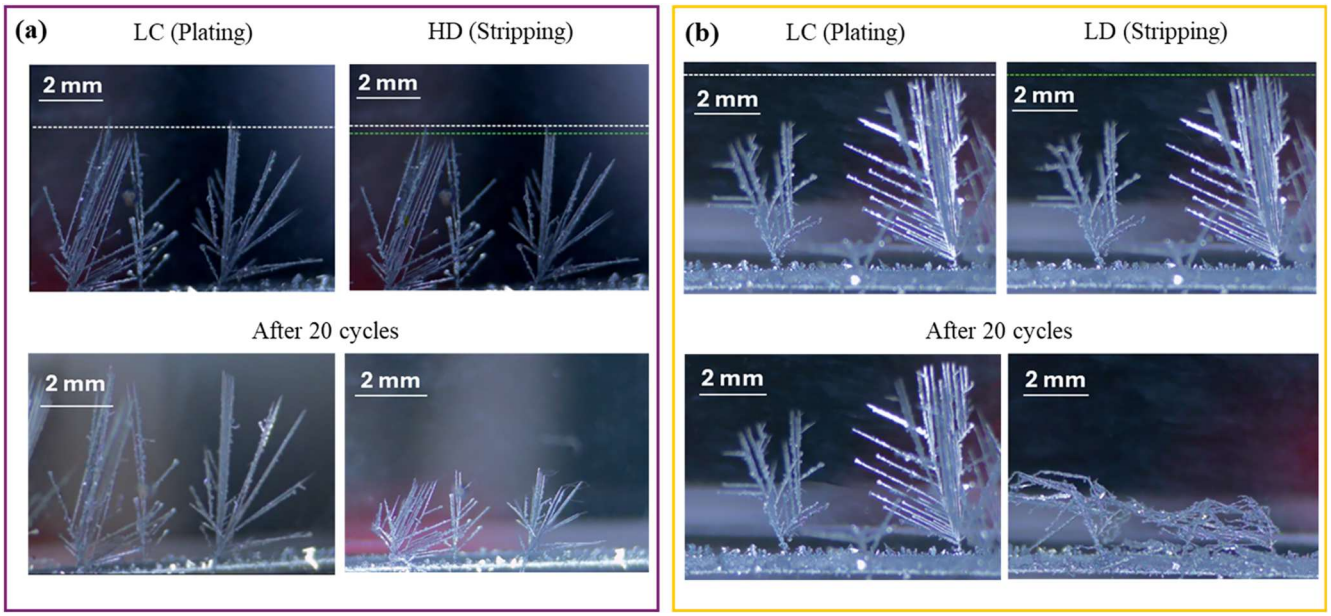

Figure 3. In-operando imaging of symmetric cell cycling for initial and after 20 plating-stripping cycles. (a) HD-LC protocol cell, dendrites after plating at 5 mA cm^{-2} and stripping at 500 mA cm^{-2}. (b) LD-LC protocol cell, dendrites after plating at 5 mA cm^{-2} and stripping at 5 mA cm^{-2}. All images were processed to scale and rotated 90° to the right such that gravity points to the left of the image.

in a uniform profile. Therefore, this work demonstrates that, just by controlling the cathode current, it is possible to manipulate the anode-electrolyte interface. This has larger implications in the sense that, the control of surface profiles at the anode-electrolyte interface may be possible by simply providing high current pulses. Surface irregularities can be dangerous in nature, providing preferential sites for successive plating for metal ions. Eventually they grow into dendrites compromising the safety of batteries with risks such as separator penetration and short circuits. These results show a promising approach by which control of irregularities on the interface is possible with applied current.

Model limitations.—It is noted that the simulation domain represents only a tiny region at the tip of the dendrite and does not represent the whole of the dendrite as shown in experiments, but it provides sufficient insight into the evolution of electrode-electrolyte interface during plating/stripping operation. We want to emphasize the fact that even the simplest possible 2D model presented here is computationally challenging and adding complexity to gain fidelity with experiments needs careful implementation of physics and boundary conditions. For more detailed discussion about the plating/stripping process inclusion of concentration evolution, surface tension, anisotropy in the electrolyte domain is necessary and will be planned as future studies.

Conclusions and Future Perspective

A simple model presented here based on secondary current distribution coupled with moving interfaces and governed by kinetics predicted improved performance for higher current compared to lower current densities. This work proves the possibility of controlling the morphology of metal anode-electrolyte interfaces using global current at the cathode. The model studied has significant limitations with the possibility of future work includes tertiary current distribution (adding concentration gradients) with dilute and concentrated solution theory, addition of anisotropy and surface tension etc. Additional physics can elucidate the mechanisms of global current regulation and provides an insight potentially impactful for the development of next-generation battery management systems (BMS). The modeling landscape in this domain remains vast and significantly underexplored. It should be noted that addition of above-mentioned physics should be sufficiently modified to accurately capture dendrite fracture, deformation, or mechanical detachment phenomena observed in LD-LC experimental results.

A critical question that arises is: what constitutes the optimal model for a given system? The answer resides in the model's predictive power and its robustness in quantitatively capturing phenomena such as void formation, dendrite growth, and other degradation pathways. Another important observation is the considerable numerical complexity associated with two-dimensional moving boundary models. Despite their relative conceptual simplicity, these models pose significant computational challenges. Our implementation of such a model in *COMSOL™ Multiphysics* serves as a demonstrative case, and the model is available upon request. A robust open-access *Maple* code version will also be hosted for accessibility.

The treatment of moving boundaries and the numerical strategies employed to solve the governing equations in two spatial dimensions (x, y) and time were found to significantly influence the efficiency and stability of the solution algorithm. The current model initiates growth from a single seed and extending the framework to represent a fully defined spatial domain or to include three-dimensional geometries would substantially increase complexity. Such an extension would necessitate the adoption of advanced numerical techniques to ensure computational feasibility within reasonable time frames. Future work from our group will explore subtle challenges and opportunities arising from alternative model formulation strategies such as phase-field, ALE, and level set methods discretized via finite element and finite volume approaches in space, coupled with optimal time integration schemes tailored to the model presented in this paper.

Acknowledgments

The authors acknowledge financial support from the National Science Foundation (NSF) Materials Research Science and Engineering Center (MRSEC, DMR-2308817), the National Science and Technology Council (NSTC) of Taiwan under contract no. NSTC 111-2221-E-007-006-MY3, the Graduate Students Study Abroad Program under contract no. NSTC 113-2917-I-007-011, and the University of Texas Science and Technology Acquisition and Retention (STARs) Fund. The authors gratefully acknowledge the Center for Electrochemistry, University of Texas at Austin, for providing partial financial support for this work through the Bard

CEC Student Scholar Fellowship under Grant no. H-F-0037 facilitated by the Welch Foundation. The information, data, or work presented herein (for the modeling and simulation) was funded by the Office of Energy Efficiency and Renewable Energy (EERE), U.S. Department of Energy, under Award Number DE-EE0011166. We sincerely thank Dr Vishnu Sundaresan, Program Manager of the DARPA MINT initiative, for inspiring this work.

ORCID

Tushar K. Telmasre https://orcid.org/0000-0002-7389-029X
Lubhani Mishra https://orcid.org/0000-0003-2135-9381
Wen-Yang Jao https://orcid.org/0009-0009-2920-369X
Aakriti Aggarwal https://orcid.org/0009-0004-8972-0625
J.-X. Kent Zheng https://orcid.org/0000-0002-0673-0560
Venkat R. Subramanian https://orcid.org/0000-0002-2092-9744

References

1. V. Ramadesigan, P. W. C. Northrop, S. De, S. Santhanagopalan, R. D. Braatz, and V. R. Subramanian, "Modeling and simulation of lithium-ion batteries from a systems engineering perspective." *J. Electrochem. Soc.*, **159**, R31 (2012).
2. F. Brosa Planella et al., "A continuum of physics-based lithium-ion battery models reviewed." *Progress in Energy*, **4**, 042003 (2022).
3. S. E. J. O'Kane et al., "Lithium-ion battery degradation: how to model it." *Phys. Chem. Chem. Phys.*, **24**, 7909 (2022).
4. R. Wang, W. Cui, F. Chu, and F. Wu, "Lithium metal anodes: present and future." *Journal of Energy Chemistry*, **48**, 145 (2020).
5. B. Liu, J. G. Zhang, and W. Xu, "Advancing lithium metal batteries." *Joule*, **2**, 833 (2018).
6. D.-H. Liu et al., "Developing high safety Li-metal anodes for future high-energy Li-metal batteries: strategies and perspectives." *Chem. Soc. Rev.*, **49**, 5407 (2020).
7. J. Liu et al., "Pathways for practical high-energy long-cycling lithium metal batteries." *Nat. Energy*, **4**, 180 (2019).
8. T. Jang et al., "Towards real-time simulation of two-dimensional models for electrodeposition/stripping in lithium-metal batteries." *ECS Trans.*, **104**, 131 (2021).
9. K. Shah et al., "Editors' Choice—Perspective—Challenges in moving to multiscale battery models: where electrochemistry meets and demands more from math." *J. Electrochem. Soc.*, **167**, 133501 (2020).
10. L. Mishra et al., "Perspective—mass conservation in models for electrodeposition/stripping in lithium metal batteries." *J. Electrochem. Soc.*, **168**, 092502 (2021).
11. W.-Y. Jao et al., *Fast Discharging Stabilizes Electrochemical Interfaces: Achieving Close-to-Unity Reversibility in 'Dendrite-Forming' Battery Electrodes* (2025), 10.26434/chemrxiv-2025-m872d.
12. W.-Y. Jao et al., *Dendritic Growth in Battery Anodes: On the Hidden Role of Crystallographic Anisotropy at Propagating Electrochemical Interfaces* (2025), 10.26434/chemrxiv-2025-tsf82-v2.